

Performance improvement of metal hydride hydrogen storage reactors by using phase change materials

Yang Ye, Weilong Wang*, Jianfeng Lu, Jing Ding

School of Materials Science and Engineering, Sun Yat-Sen University, China

Corresponding author: Weilong Wang, wwlong@mail.sysu.edu.cn

Abstract

The hydrogen absorption of metal hydride (MH) is an exothermic process. For a cylindrical MH hydrogen storage reactor with a concentric tube heat exchange, the hydrogen adsorption heat is discharged by the heat transfer fluid (HTF), and the absorption reaction proceeds along the radial direction from the center to the periphery, which leads to the non-uniformity of the reaction process and limits the average reaction rate. In order to improve the hydrogen storage rate, the phase change material (PCM) is used to assist in heat transfer by surrounding the reactor. This paper establishes a mathematical model to describe the heat and mass transfer process within the reactors. The results show that the surrounding PCM can absorb the reaction heat at the periphery of the reactor, and promote the reaction proceeding in this region. Thus, the average hydrogen absorption rate of the reactor surrounded by PCM is increased by about 1.5 times owing to the assisted heat transfer of PCM.

Keywords: Metal hydride, Hydrogen storage, Phase change materials, Heat transfer fluid, Heat transfer

Nonmenclature

Abbreviations

MH	Metal hydride
HTF	Heat transfer fluid
PCM	Phase change material

Symbols

C	reaction rate constant, s^{-1}
c_p	specific heat, $J/(kg \cdot K)$

E	activation energy, $J/(mol \cdot K)$
f	liquid fraction of PCM
L	latent heat of PCM, J/kg
M	molecular weight, kg/mol
P	pressure, MPa
R	universal gas constant, $J/(mol \cdot K)$
T	temperature, K
u	velocity, m/s
wt	gravimetric storage capacity
x	reacted fraction
ΔH	reaction enthalpy, J/mol
ΔS	reaction entropy, $J/(mol \cdot K)$
ε	porosity
λ	thermal conductivity, $W/(m \cdot K)$
μ	dynamic viscosity, $Pa \cdot s$
ρ	density, kg/m^3

Subscripts

O	initial
e	effective value
g	gas
h	heat transfer fluid
in	inlet
liq	liquefaction
m	magnesium hydride
p	Phase change material
ref	reference
sol	solidification

1. Introduction

Hydrogen is an environment-friendly secondary energy, which has been used as an energy carrier to deal with the site-specific and intermittent of renewable energy [1]. As a fuel, hydrogen has the advantages of high calorific value and zero emission. One of the difficulties in large-scale application of hydrogen is the safe and efficient hydrogen storage. Compared with gas-state and liquid-state hydrogen storage, metal hydride (MH) hydrogen storage has higher volume hydrogen storage capacity, and it is more safe and reliable [2]. Among MHs, magnesium hydride (MgH_2) is considered to be the most promising solid hydrogen storage material with high gravimetric hydrogen storage capacity (7.6 %wt) [3].

The hydrogen absorption and desorption process of MH is accompanied by thermal effects. The reaction enthalpy of MgH_2 is as high as 75 kJ/mol. Thus, the hydrogen storage performance is closely related to the heat and mass transfer of MH hydrogen storage reactor [4]. In most of the research, the reaction heat of absorption is discharged from the reaction bed by heat transfer fluid (HTF) through a variety of heat exchangers, such as straight tube heat exchangers [5,6], helical coil heat exchangers [7,8] and microchannel heat exchangers [9]. With the complexity of the heat exchangers, the hydrogen absorption rate is significantly increased due to the larger heat transfer area. However, due to the heat release in the hydrogen absorption process, the reaction first proceeds near the heat exchangers. In the place far away from the heat exchangers, the reaction will be limited for a long time until the temperature drops. Although multiple heat exchangers can be installed at different locations [6], this undoubtedly increases the complexity of the reactor and reduces the stability of operation.

For a cylindrical reactor with a concentric straight tube heat exchange (MH-HTF reactor), the hydrogen absorption reaction proceeds along the radial direction from the center to the periphery, which leads to the non-uniformity of the reaction and limits the average reaction rate [5]. Thus, this paper proposes a new method of using PCM (surrounding the reactor) to assist in heat transfer for the MH-HTF reactor (MH-HTF-PCM reactor). Using PCM to discharge the heat does not require additional pumping of HTF, which ensures the stability of the system. Moreover, due to the large latent heat advantage of the PCM, the heat absorbed during absorption process can be used as the heat source for the hydrogen desorption process, which

improves the energy utilization of the storage system [10].

In order to study the effect of PCM assisted heat transfer on the performance of the reactor, this paper establishes a two-dimensional mathematical model to describe the heat and mass transfer process within the reactors. The model validation is verified by the experimental results in the previous literature. Compared with the MH-HTF reactor, detailed results are presented concerning the evolution of the temperature and reaction conversion rate of the new MH-HTF-PCM reactor.

2. Mathematical model

The traditional hydrogen storage reactor is shown in Fig. 1a (MH-HTF reactor). Several MH compacted disks, made of Mg/MgH_2 and expanded graphite, are stacked in a cylindrical stainless steel tank. A straight tube heat exchanger is inserted in the center of the reactor. In the process of hydrogen absorption, the reaction heat is discharge by the heat transfer fluid (synthetic oil of Dowtherm A) in the tube. Due to the symmetry of the reactor, a two-dimensional and half of the reactor can be used as a computational domain. In order to overcome the long-time reaction limitation in the reactor far away from the tube heat exchange, PCM is used to surround the reactor to assist in heat transfer as shown in Fig. 1b (MH-HTF-PCM reactor). Sodium nitrate (NaNO_3) is selected as PCM due to its suitable melting point (580.0 K) and high latent heat [11]. Similarly, the new reactor is simplified to a half of two-dimensional symmetry plane. In order to establish the mathematical model of the heat and mass transfer within the reactors, the assumptions are as follows:

- (a) There is a local thermal equilibrium between the gas and solid phase in the porous medium [12].
- (b) The reactors has good thermal insulation.
- (c) The hydrogen is considered as an ideal gas, and its pressure is uniform in the bed [13].
- (d) The thermos-physical properties of MH, HTF and PCM are constant.
- (e) The convection of liquid PCM is negligible due to the heat transfer through PCM is mainly by heat conduction [14].

2.1. Governing equations

For MH beds, the reaction equilibrium temperature and pressure are determined by the Van't Hoff equation [4]:

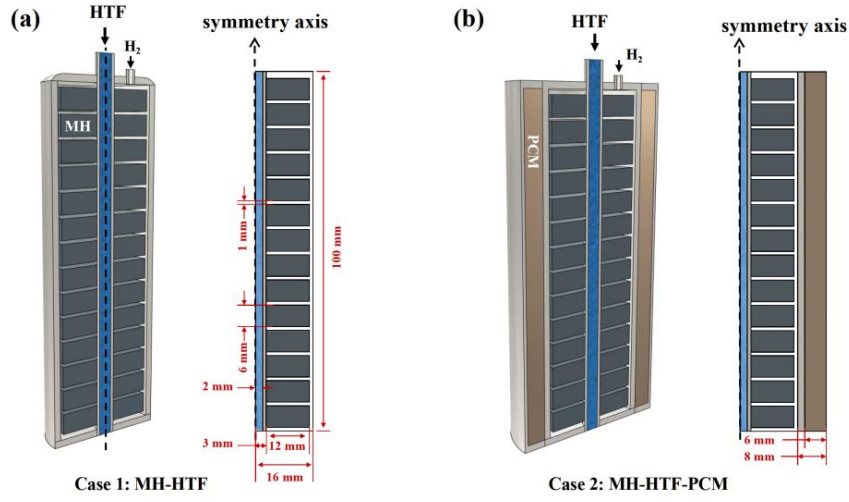


Fig. 1. (a) The cylindrical reactor with a concentric tube heat exchange (Case 1: MH-HTF); (b) the new reactor surrounded by the PCM (Case 2: MH-HTF-PCM)

$$\ln \frac{p_{eq}}{p_0} = \frac{\Delta H}{RT_m} - \frac{\Delta S}{R} \quad \text{where } P_0 = 0.1 \text{ MPa} \quad (1)$$

Energy equation of MH beds [5]:

$$\rho \cdot c_p \cdot \frac{\partial T_m}{\partial t} + \rho_g \cdot c_{p,g} \cdot \nabla(T_m \cdot \vec{V}_r) = \lambda_e \cdot \nabla^2 T_m + S \quad (2)$$

Where the effective thermal conductivity λ_e , effective volumetric heat capacity $\rho_g \cdot c_p$ and heat source S are as follows:

$$\lambda_e = \varepsilon \cdot \lambda_g + (1 - \varepsilon) \cdot \lambda_m \quad (3)$$

$$\rho \cdot c_p = \varepsilon \cdot \rho_g \cdot c_{p,g} + (1 - \varepsilon) \cdot \rho_m \cdot c_m \quad (4)$$

$$S = \frac{\rho_m \cdot wt \cdot (1 - \varepsilon)}{M} \cdot \frac{dx}{dt} \cdot \Delta H \quad (5)$$

Reaction kinetic equations for hydrogen absorption process is expressed by Chaise et al [13].

$$\frac{dx}{dt} = C \exp\left(-\frac{E}{R \cdot T_m}\right) \cdot \left(\frac{P_g}{P_{eq}} - 1\right) \cdot \frac{x - 1}{2 \ln(1 - x)} \quad P_g > 2P_{eq} \quad (6)$$

$$\frac{dx}{dt} = C \exp\left(-\frac{E}{R \cdot T_m}\right) \cdot \left(\frac{P_g}{P_{eq}} - 1\right) \cdot (1 - x) \quad P_{eq} < P_g < 2P_{eq} \quad (7)$$

For HTF, continuity, momentum and Energy equations are as follows [15]:

$$\nabla \cdot \vec{u} = 0 \quad (8)$$

$$\rho_h \frac{\partial \vec{u}}{\partial t} + \rho_h (\vec{u} \cdot \nabla) \vec{u} = -\nabla P + \mu_h \nabla^2 \vec{u} \quad (9)$$

$$\rho_h c_{p,h} \frac{\partial T_h}{\partial t} + \rho_h c_{p,h} \vec{u} \cdot \nabla T = \lambda_h \cdot \nabla^2 T_h \quad (10)$$

For PCM, the energy equation based on the enthalpy formulation are as follows [11]:

$$\frac{\partial H}{\partial t} = \nabla \cdot (\lambda_p \nabla(T_p)) \quad (11)$$

Where H is the sum of sensible heat:

$$H(T_p) = \int_{T_{liq}}^{T_p} \rho_p c_{p,p} dT_p + \rho_p \cdot L \cdot f(T_p) \quad (12)$$

The liquid fraction f based on volume can be defined as follows:

$$f = \begin{cases} 0 & T_p \leq T_{sol} \\ (T_p - T_{sol}) / (T_{liq} - T_{sol}) & T_{sol} \leq T_p \leq T_{liq} \\ 1 & T_p \geq T_{liq} \end{cases} \quad (13)$$

2.2 Initial and boundary conditions

The initial temperature of MH and PCM and hydrogen supply pressure are as follows:

$$T_{m,o} = T_{p,o} = 573.0 \text{ K} \quad (14)$$

$$P_g = \begin{cases} P_0 + (P_{in} - P_0)t/10 & t < 10 \text{ s} \\ P_{in}, 1.0 \text{ MPa} & t \geq 10 \text{ s} \end{cases} \quad (15)$$

Inlet velocity of HTF is 1.0 m/s, and the inlet temperature is 573 K.

The adiabatic and symmetry boundary conditions:

$$\nabla T \cdot \vec{n} = 0 \quad (16)$$

Heat transfer boundary:

$$\lambda \frac{\partial T}{\partial \vec{n}} = h_f \Delta T \quad (17)$$

2.3. Model validation

The above equations are solved by Fluent 14.5. For the reactor without PCM, the simulation results are compared with the experimental results reported by Chaise et al [13]. in Fig. 2a. For the reactor surrounded by PCM, the simulation results are compared with the experimental results by Garrier et al. in Fig. 2b [14]. The simulation results of temperatures, average conversion rate or hydrogen absorbed volume ratio of the MH bed during the absorption process have an agreement with the experimental data. Thus, the mathematical model is valid for the above hydrogen storage reactors.

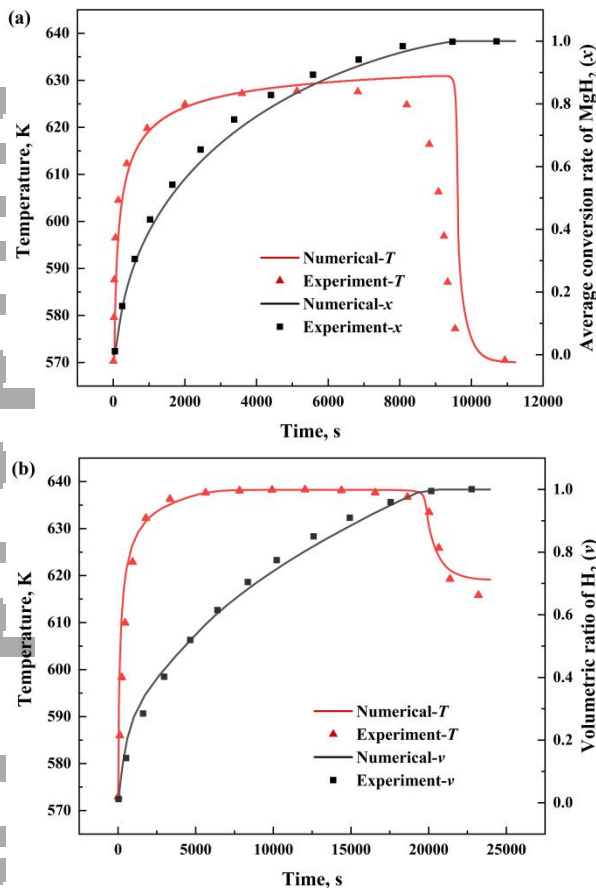


Fig. 2. Comparison of simulation results with experimental results reported by (a) Chaise et al. [13] and (b) Garrier et al. [14]

3. Results and discussion

The physical parameters of MH, HTF, PCM and H₂ are listed in Table 1 [5,11,13].

Table 1

Physical parameters of MH, HTF, PCM and H₂.

MH (Mg/MgH ₂ + EG)	PCM (NaNO ₃)
$\rho_m = 1800 \text{ kg/m}^3$	$\rho_p = 2260 \text{ kg/m}^3$
$c_{p,m} = 1545 \text{ J/(kg} \cdot \text{K)}$	$c_{p,p} = 1820 \text{ J/(kg} \cdot \text{K)}$
$\lambda_m = 2 \text{ W/(m} \cdot \text{K)}$	$\lambda_p = 0.48 \text{ W/(m} \cdot \text{K)}$
$\varepsilon = 0.4$	$L = 174000 \text{ J/kg}$
$wt = 0.05$	$T_{sol} = 580.0 \text{ K}$
$\Delta H = -75000 \text{ J/mol}$	$T_{lid} = 581.0 \text{ K}$
$\Delta S = -135.6 \text{ J/(K} \cdot \text{mol)}$	
$E = 130000 \text{ J/(K} \cdot \text{mol)}$	
$C = 10^{10} \text{ s}^{-1}$	
H ₂	HTF (Dowtherm A)
$c_{p,g} = 14000 \text{ J/(kg} \cdot \text{K)}$	$\rho_h = 810 \text{ kg/m}^3$
$\lambda_g = 0.24 \text{ W/(m} \cdot \text{K)}$	$c_{p,h} = 2350 \text{ J/(kg} \cdot \text{K)}$
$\mu_g = 8.9 \times 10^{-6} \text{ Pa} \cdot \text{s}$	$\lambda_h = 0.094 \text{ W/(m} \cdot \text{K)}$
$M = 0.002 \text{ kg/mol}$	$\mu_h = 2.15 \times 10^{-4} \text{ Pa} \cdot \text{s}$

For the two reactors, the initial temperature of MH and PCM is 573.0 K, the hydrogen absorption pressure is 1.0 MPa, the inlet velocity of HTF is 1.0 m/s, and the inlet temperature of HTF is 573.0 K. Fig. 3 shows the temperature and MgH₂ distribution during hydrogen absorption process of the two reactors. For the MH-HTF reactor in Fig. 3a, the MH temperature increases rapidly in the initial stage of the reaction. As HTF continuously discharges the absorption heat, the temperature of MH first decreases near the tube heat exchange. But, the temperature far away from the concentric tube remains high for a long time. The hydrogen absorption reaction proceed along the radial direction from the periphery of the tube to the temperature decreasing direction (Fig. 3b), which leads to the non-uniformity of the reaction and limits the average reaction rate. Compared with the MH-HTF reactor, the surrounded PCM assist in absorbing the reaction heat mainly by its latent heat. As shown in Fig. 3a, the temperature at the side far away from the tube heat exchange decreases obviously due to the heat transfer form MH to PCM, and the combined heat transfer of HTF and PCM accelerates the heat discharge of MH. As a result in Fig. 3b, the hydrogen absorption reaction takes place in the center and periphery of the reaction bed at the same time, which greatly accelerates the absorption process.

Fig. 4 shows the comparison of the average temperature of MH bed and the conversion rate of MgH₂ in the hydrogen absorption process. For both MH-HTF and MH-HTF-PCM reactors, in the initial stage of the reaction, the average temperature of MH bed

rapidly increases to 644.0 K, which is the reaction equilibrium temperature at 1.0 MPa, and then the temperature gradually decreased with the discharge of the absorption heat. Due to the assistance of PCM, the average temperature of MH bed in the MH-HTF-PCM

reactor drops faster. In Fig. 4b, the hydrogen absorption time of MH-HTF and MH-HTF-PCM reactors is 3230 s and 1284 s respectively, and the average absorption rate is increased by 1.5 times owing to the assisted heat transfer of PCM.

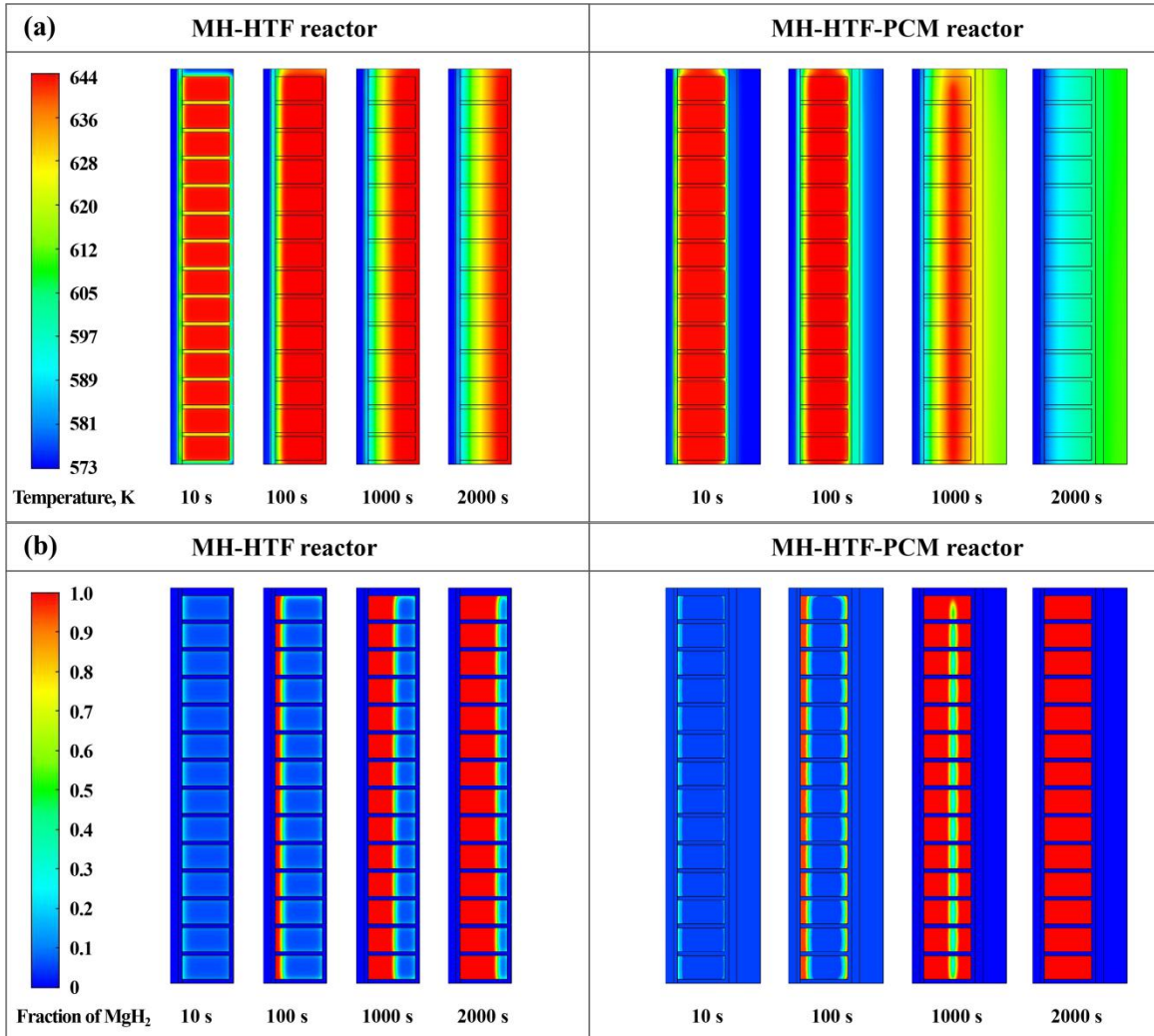


Fig. 3. Distribution of the (a) temperature and (b) fraction of MgH_2 for the MH-HTF and MH-HTF-PCM reactor in the hydrogen absorption process.

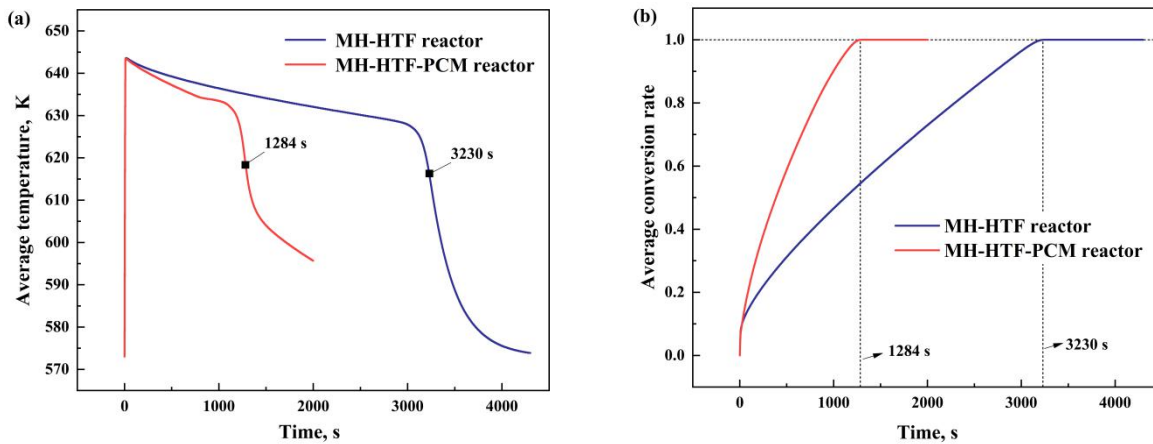


Fig. 4. Comparison of (a) average temperature and (b) average conversion rate of MgH_2 during the hydrogen absorption process.

4. Conclusions

This paper proposes a new method of using PCM (surrounding the reactor) to assist in heat transfer for a cylindrical hydrogen storage reactor with a concentric tube heat exchanger (MH-HTF reactor). A valid mathematical model is established to describe the heat and mass transfer process within the reactors. Compared with the MH-HTF reactor, the surrounded PCM can absorb the reaction heat at the periphery of the reactor, and promote the reaction proceeding in this region. The hydrogen absorption time of MH-HTF and MH-HTF-PCM reactors is 3230 s and 1284 s respectively, and the average absorption rate is increased by 1.5 times owing to the assisted heat transfer of PCM.

Acknowledgements

This work was founded by the National Natural Science Foundation of China (51976237), National Key Research and Development Project (2018YFB1501003), Science and Technology Planning Project of Guangdong Province (2015A010106006).

References

- [1] Mazloomi K, Gomes C. Hydrogen as an energy carrier: Prospects and challenges. *Renew Sustain Energy Rev* 2012;16:3024 – 33.
- [2] Barthelemy H, Weber M, Barbier F. Hydrogen storage: Recent improvements and industrial perspectives. *Int J Hydrogen Energy* 2017;42:7254 – 62.
- [3] Rusman NAA, Dahari M. A review on the current progress of metal hydrides material for solid-state hydrogen storage applications. *Int J Hydrogen Energy* 2016;41:12108 – 26.
- [4] Afzal M, Mane R, Sharma P. Heat transfer techniques in metal hydride hydrogen storage: A review. *Int J Hydrogen Energy* 2017;42:30661 – 82.
- [5] Bao Z, Yang F, Wu Z, Cao X, Zhang Z. Simulation studies on heat and mass transfer in high-temperature magnesium hydride reactors. *Appl Energy* 2013;112:1181 – 9.
- [6] Bao Z, Wu Z, Nyamsi SN, Yang F, Zhang Z. Three-dimensional modeling and sensitivity analysis of multi-tubular metal hydride reactors. *Appl Therm Eng* 2013;52:97 – 108.
- [7] Wu Z, Yang F, Zhang Z, Bao Z. Magnesium based metal hydride reactor incorporating helical coil heat exchanger: Simulation study and optimal design. *Appl Energy* 2014;130:712 – 22.

- [8] Dhaou H, Ben Khedher N, Mellouli S, Souahlia A, Askri F, Jemni A, et al. Improvement of thermal performance of spiral heat exchanger on hydrogen storage by adding copper fins. *Int J Therm Sci* 2011;50:2536 – 42.
- [9] Li H, Wang Y, He C, Chen X, Zhang Q, Zheng L, et al. Design and performance simulation of the spiral mini-channel reactor during H₂ absorption. *Int J Hydrogen Energy* 2015;40:13490 – 505.
- [10] Ye Y, Lu J, Ding J, Wang W, Yan J. Numerical simulation on the storage performance of a phase change materials based metal hydride hydrogen storage tank. *Appl Energy* 2020;278:115682.
- [11] Mellouli S, Abhilash E, Askri F, Ben Nasrallah S. Integration of thermal energy storage unit in a metal hydride hydrogen storage tank. *Appl Therm Eng* 2016;102:1185 – 96.
- [12] Ben Mâad H, Miled A, Askri F, Ben Nasrallah S. Numerical simulation of absorption-desorption cyclic processes for metal-hydrogen reactor with heat recovery using phase-change material. *Appl Therm Eng* 2016;96:267 – 76.
- [13] Chaise A, De Rango P, Marty P, Fruchart D. Experimental and numerical study of a magnesium hydride tank. *Int J Hydrogen Energy* 2010;35:6311 – 22.
- [14] Garrier S, Delhomme B, De Rango P, Marty P, Fruchart D, Miraglia S. A new MgH₂ tank concept using a phase-change material to store the heat of reaction. *Int J Hydrogen Energy* 2013;38:9766 – 71.
- [15] Yang X, Yu J, Xiao T, Hu Z, He YL. Design and operating evaluation of a finned shell-and-tube thermal energy storage unit filled with metal foam. *Appl Energy* 2020;261:114385.